Cluster nanoplasmas in strong FLASH pulses: formation, excitation and relaxation

Ulf Saalmann

Max Planck Institute for the Physics of Complex Systems, Nöthnitzer Straße 38, 01187 Dresden, Germany
and
Max Planck Advanced Study Group at the Center for Free-Electron Laser Science, Luruper Chaussee 149, 22761 Hamburg, Germany

E-mail: us@pks.mpg.de

Abstract
Clusters exposed to intense laser radiation quickly turn into nanoplasmas: short-lived electron plasmas confined by the charged cluster ions on a nanometre scale. Although the cluster will eventually explode, the transient multi-electron dynamics during the pulse is of great interest and largely unexplored. It determines the mechanism of energy absorption and thus may help to understand measured electron and ion spectra, also in other samples, such as large molecules. Furthermore, an experimental setup with short pulses and access to observables, which becomes possible because of the sample's finite size, offers novel possibilities of investigating the non-equilibrium dynamics of plasmas. Here, the formation, excitation and relaxation of nanoplasmas in rare-gas clusters driven by strong pulses from free-electron lasers (FELs) with photon frequencies in the range of about 10 to 100 eV as currently available at FLASH are discussed. It is the unique combination of brilliant, tunable and short-pulse radiation in this machine and upcoming x-ray FELs which makes such studies feasible.

(Some figures in this article are in colour only in the electronic version)

1. Introduction

Since the very first measurements (Wabnitz *et al* 2002), clusters have been prominent targets (Bostedt and Möller 2010) for studies with intense vacuum (VUV) and extreme (XUV) ultraviolet radiation as available from the first short-wavelength free-electron laser (FEL) FLASH (Ackermann *et al* 2007). They are prototypes for finite systems with the exclusive feature that their size can be easily changed from a few atoms, as in small molecules, to a few million atoms, as in micro-droplets. Clusters can be made up of atoms or molecules. Here we restrict ourselves to rare-gas clusters since many experiments are performed with this cluster type. The corresponding inter-atomic distances are a few angstroms, just like in molecules. The binding, which is due to van der Waals interactions (Haberland 1994), however, is much weaker and hardly changes the electronic structure of the atoms.

The response of such rare-gas clusters to intense pulses at near-infrared (NIR) frequencies has been extensively studied and recently reviewed (Krainov and Smirnov 2002, Saalmann *et al* 2006). Experiments in the VUV and XUV regime became feasible by the advent of FLASH (Bostedt *et al* 2009) and very recently by the SPring-8 Compact SASE Source (Fukuzawa *et al* 2009). First cluster experiments with x-ray pulses are currently under way at the LCLS. In all cases a plasma confined to the cluster volume can be formed. Its characteristics, such as density and temperature, depend crucially on the laser radiation and may change strongly on a femtosecond time scale, either due to the absorption of energy from the laser or due to particle and light emission. The observation of fast electrons (Springate *et al* 2003), highly charged ions (Ditmire *et al* 1997) or high-energy photons (McPherson *et al* 1994) has been strongly driving the interest in laser–cluster interaction for NIR radiation. FEL sources with shorter wavelengths can

induce nanoplasma formation under novel conditions. The possibility of creating and driving such finite and 'open' plasmas allows us to study non-equilibrium multi-electron dynamics, eventually down to a sub-femtosecond time scale (Saalmann *et al* 2008).

First, we present a qualitative picture of clusters in strong laser pulses and introduce relevant quantities that characterize the laser–cluster interaction (section 2). Basic processes, such as photo-absorption and collisions, occur in strongly excited multi-electron systems which makes a quantitative theoretical description challenging. We discuss two approaches to this problem (section 3). By means of these approaches, many theoretical studies have been performed in order to understand measurements done at FLASH over the last 8 years. We report a few of them and discuss the main conclusions (section 4). We finish with an outlook on new directions of FEL-cluster experiments and a recent theoretical proposal for interesting measurements (section 5).

We do not present a review covering all aspects of the theoretical description of atomic clusters exposed to intense radiation from VUV/XUV FELs such as FLASH. Rather, we discuss the basic mechanisms and present some of the theoretical methods which aim at a quantitative treatment of the induced nanoplasma dynamics.

2. Clusters in strong laser fields

Before quantifying the laser impact, we briefly outline the general scenario of the cluster dynamics driven by intense laser irradiation. For the moment, we consider the laser pulse to be strong, irrespective of its frequency ω, if it leads to multiple ionization of the atoms in the cluster. Due to the large number of atoms initially bound in the cluster, this ionization may result in a very highly charged system. With the number of atoms in the cluster N and an average ionic charge q, the cluster charge becomes $Q = Nq$, resulting in an extended and strongly attractive potential, cf figure 1 showing its formation. It is this potential which makes the response of clusters to strong laser pulses qualitatively different from that of atoms or small molecules. The two most important implications for the electron dynamics in clusters exposed to short-wavelength radiation, to be discussed below in detail, are

(i) trapping of electrons which may form a plasma, usually referred to as nanoplasma (Ditmire *et al* 1996), which dominates the cluster dynamics and

(ii) charging of atoms/ions, in particular, at the cluster surface, through 'field' ionization (Gnodtke *et al* 2009).

The plasma formation implies various secondary processes, such as electron-impact ionization, equilibration through electron–electron collisions and expansion due to hydrodynamic pressure. Note that both effects, plasma formation and secondary processes, depend on the instantaneous cluster potential which changes in time due to two counteracting processes. On one hand, it becomes deeper due to further excitation of bound electrons into the plasma (cf figure 1(b)). On the other hand, the potential expands and becomes shal-

lower because of the expansion of the cluster[1] (cf figure 1(c)). The expansion dynamics have been hardly investigated in the context of FEL–cluster interaction.

2.1. Transition from NIR to x-ray frequencies

The intensity I of the incoming laser pulse alone is not sufficient to quantify its impact on the electrons in the cluster atoms. Rather, the frequency ω of the laser is another key parameter, which is even relevant for non-resonant processes. It is known from the atoms (Faisal 1987) that ionization processes can be treated in perturbation theory as long as the ponderomotive shift,

$$E_{\text{pond}} = I/4\omega^2, \tag{1}$$

which occurs mainly for the final (continuum) states but not for the initial (bound) state, is small compared to the frequency ω, i.e. as long as $E_{\text{pond}} \ll \omega$ or $I \ll 4\omega^3$ (Joachain *et al* 2000). If not specified otherwise, we assume atomic units. Clearly, perturbation theory can be used for much higher intensities I if the frequency ω is large. To be specific, for frequencies of $\hbar\omega = 10$ eV and 100 eV, perturbation theory applies for $I \ll 7 \times 10^{15}$ W cm^{-2} and $I \ll 7 \times 10^{18}$ W cm^{-2}, respectively. Within this picture, electrons are released through the absorption of a single photon or a few photons. The picture changes qualitatively if the frequency becomes so small that a laser period is long compared to typical times of electron motion. In this case, the interaction is strong at maximal electric fields which can be considered quasi-static. The electron may tunnel through the barrier or, for very high fields, leave the atom/ion above the barrier. The parameter which distinguishes the regimes of single-/multi-photon and tunnelling ionization was introduced by Keldysh (1965), $\gamma = \sqrt{E_{\text{bind}}/2E_{\text{pond}}}$, with $\gamma < 1$ being an indicator for tunnelling ionization. Thus, the process by which electrons are excited into the plasma, sometimes referred to as 'inner ionization' (Last and Jortner 1999), strongly depends on the laser frequency (Saalmann *et al* 2006).

Correspondingly, 'outer ionization', which refers to the loss of electrons from the nanoplasma, differs for NIR and VUV/XUV frequencies. In order to quantify the importance of the laser, one may use the quiver amplitude,

$$x_{\text{quiv}} = \sqrt{I}/\omega^2, \tag{2}$$

characterizing the amplitude of free-electron motion in an oscillating field defined by I and ω. This length has to be compared to the cluster size. Quiver amplitudes for a

---

[1] The expansion dynamics have been measured for NIR frequencies by means of pump–probe experiments (Zweiback *et al* 1999) and discussed within a macroscopic model (Ditmire *et al* 1996) and microscopic calculations (Saalmann and Rost 2003, Saalmann 2006). Here, the energy absorption is most efficient when the eigenfrequency of the cluster potential becomes resonant with the laser frequency (Saalmann and Rost 2003). For quasi-neutral clusters, this frequency coincides with the frequency of a spherical plasma $\omega_{\text{pl}} = \sqrt{4\pi\varrho_{\text{el}}/3}$ (Ditmire *et al* 1996). This resonant collective absorption makes clusters extremely reactive for certain delays between the pump and probe pulse; almost 100 % absorption of the incoming light has been measured (Zweiback *et al* 1999). Of course, the absolute value depends also on the target size and target density.
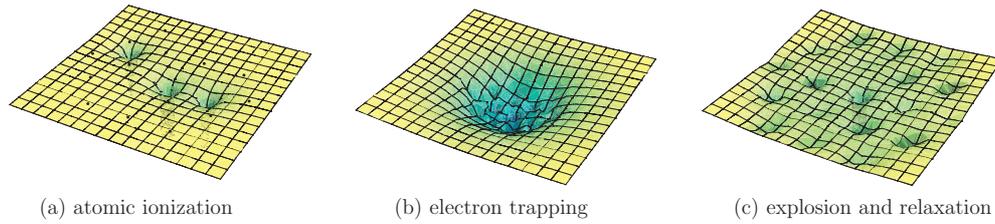
Figure 1. Sketch of the cluster potential as a function of time. For convenience we show a 2D system. (a) The firstly ionized electrons see only single atomic potentials which are not influenced by the other cluster atoms marked by black dots. (b) Further ionization leads to one extended, deep cluster potential in which the electron plasma is trapped. (c) The cluster potential disintegrates due to expansion; inter-atomic barriers are raised.

typical intensity of $I = 10^{14}$ W cm^{-2} and the two frequencies ω considered above are about 0.2 Å and 0.002 Å, respectively, and thus much smaller than the clusters with diameters of a few nanometres[2]. Therefore, energy absorption occurs 'locally' at individual atoms/ions. The two relevant processes are discussed in subsection 4.1.

2.2. Electron trapping in the cluster potential

Electrons released early in the pulse from their 'mother' atom leave the cluster (cf figure 1(a)) directly. They could lose energy due to inelastic scattering on the way out. Nevertheless, recent experiments (Bostedt *et al* 2008, 2010) clearly show a peak at the energy E_{excess} expected for the ionization of single atoms. This observation agrees with the fact that in rare-gas clusters, which are bound by the van der Waals interaction, the electronic structure is only slightly modified during cluster formation. Furthermore, it indicates that inelastic scattering is less important that one would expect from the large cross sections, probably due to the small sizes of the cluster and the large fraction of atoms being at the cluster surface.

The emitted electrons leave a positively charged background behind, of which eventually further electrons cannot escape from since they do not have sufficient energy; the electrons are trapped. Such trapping reduces the overall charging (Saalmann and Rost 2002). This build-up of the trapping potential has recently been measured by photo-electron spectroscopy with argon clusters (Bostedt *et al* 2008). The onset of trapping depends on the cluster size N and the laser frequency ω. For simplicity, one may assume a spherical, homogeneously charged cluster of charge Q and radius R. The corresponding potential reads

$$V(r) = \begin{cases} -Q/R[3/2 - (r/R)^2/2] & \text{for} \quad r \leqslant R, \\ -Q/r & \text{for} \quad R \leqslant r. \end{cases} \quad (3)$$

This potential increases the binding energy E_{bind} of an electron in an atom having a distance r to the cluster centre by $V(r)$. Accordingly, the excess or final energy is reduced, $E_{excess} = [E_{bind} + V(r)] + \hbar\omega$, and can eventually become negative; the electrons are trapped. This occurs earlier for atoms at the cluster centre ($r = 0$) than at its surface ($r = R$).

---

[2] For NIR frequencies, the quiver amplitude and the cluster size are of the same order. The electron plasma is driven through the whole cluster and absorption occurs mainly 'globally' (Ditmire *et al* 1996, Saalmann and Rost 2003), which is sometimes referred to as collisionless absorption.
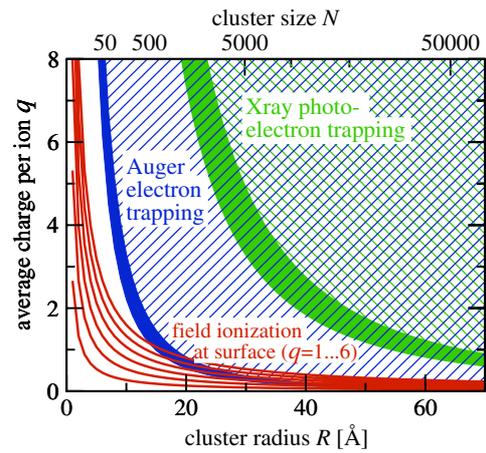

Figure 2. Electron trapping and strong-field effects of homogeneously charged neon clusters with an average charge q per ion and a cluster radius R. Trapping of electrons detached by 12 keV photons (region above and including the green/light-grey shaded band) and Auger decays (region above and including the blue/dark-grey shaded band). The thick lower borders take into account that electrons are released from any position in the cluster. Red/solid lines: ionization of surface ions at various charge states ($q = 1, \ldots, 6$) due to the internal radial field of the charged cluster estimated by the Bethe rule. Figure from Gnodtke *et al* (2009).

Figure 2 shows an overview for neon clusters with radius R and average charge $q = Q/N$ at which trapping starts to occur. The atom type fixes the cluster atomic density as well as the binding energy E_{bind}. The frequency of $\hbar\omega = 12$ keV used in this figure (Gnodtke *et al* 2009) is the high-end frequency of the upcoming European XFEL. At these high photon energies, trapping occurs only for large and highly charged clusters (green area in figure 2). Auger electrons, which in the case of neon have excess energies of about 900 eV, are trapped for much smaller and more weakly charged systems (blue area in figure 2). Obviously, at FLASH with even smaller photon energies of $\hbar\omega = 10, \ldots, 100$ eV, trapping of electrons is a very important process.

2.3. Field ionization and electron migration

From the expression for the cluster potential in equation (3), it becomes clear that there is a radial electric field $\mathcal{E}(r) = \mathrm{d}/\mathrm{d}r\, V(r)$, which is maximal at the cluster surface $r \approx R$. This applies also to situations where electrons tend to

screen the ionic charge since screening modifies the potential[3] only for the small $r < R$. The absolute value of the electric field at the surface reads

$$\mathcal{E}(R) = Q/R^2 = \sqrt[3]{N}\,q\big/r_s^2, \tag{4}$$

with the Wigner–Seitz radius $r_s = \sqrt[3]{3/4\pi\varrho_{at}}$ for an atomic density ϱ_{at}. Obviously, the field increases for the larger cluster sizes N. It can easily become strong enough in order to ionize atoms at the cluster's surface. To estimate this effect, one may compare the electric field (4) with the critical fields necessary for above-the-barrier ionization according to the so-called Bethe rule (Bethe and Salpeter 1957). Using these critical fields, which are given for the ionic charge q by $\mathcal{E}_q = E_{bind,q}{}^2\big/(4q)$, one sees from the red lines for $q = 1, \ldots, 6$ in figure 2 that this ionization process cannot be neglected. As it is similar to ionization with a static electric field, the process is termed field ionization. Note, however, that electrons released from the surface atoms in this way are always trapped in the cluster potential and become part of the nanoplasma. They migrate to the cluster centre in order to screen the positive cluster charge (Gnodtke *et al* 2009).

Finally, we again stress that, although not specified in equation (3), the trapping potential and the induced radial electric field change in time since the charge Q and radius R are time dependent, cf figure 1, which shows the disintegration of the cluster potential. The respective time scales of charging and expansion depend sensitively on the combination of cluster type and FEL radiation.

3. Theoretical methods

The very first experiments of clusters irradiated with VUV-FEL radiation by the Hamburg group (Wabnitz *et al* 2002) led to a variety of theoretical investigations, not least because of the surprisingly high ionic charge states detected. From these observations, it became clear that atoms in the clusters are multiply charged, and thus a nanoplasma has been formed. The interaction of a finite plasma with intense radiation at these frequencies had never been investigated before. Since a first-principle description of the complex ultra-fast dynamics is not possible, theoretical models, which incorporate the essential physical processes in forming and exciting the plasma, have been proposed. One may classify the approaches into those based on molecular dynamics (Siedschlag and Rost 2004, Jungreuthmayer *et al* 2005, Georgescu *et al* 2007b) and those using rate equations (Santra and Greene 2003, Walters *et al* 2006, Ziaja *et al* 2008).

---

[3] Of course, the potential depends on the instantaneous electron density. We assume that it is spherical and fully neutralizes the ion background from the centre up to the radius R_{el}. This requires an electron charge of $Q_{el} = (R_{el}/R)^3 Q_{ion}$ and the cluster net charge becomes $Q = Q_{ion} - Q_{el}$. Then the potential reads

$$V(r) = \begin{cases} -(Q/R)[3/2 - (R_{el}/R)^2/2] & \text{for} \quad r \leqslant R_{el}, \\ -(Q/R)[3/2 - (r/R)^2/2] & \text{for} \quad R_{el} \leqslant r \leqslant R, \\ -Q/r & \text{for} \quad R \leqslant r, \end{cases}$$

i.e. it is constant for $r < R_{el}$, becomes harmonic up to $r = R$ and finally Coulombic for $r > R$.

In the first group of models, classical equations of motion for (interacting) electrons and ions in the oscillating laser field are solved. The numerical propagation is trivial for small systems but requires hierarchical schemes, such as tree-codes (Barnes and Hut 1986) or fast-multipole methods (Greengard and Rokhlin 1987, Dachsel 2010), for the large particle numbers n, i.e. $n \gtrsim 10^4$. The laser becomes less important for larger frequencies since ponderomotive energy and quiver amplitude decrease, cf equations (1) and (2) and their discussion. The Coulomb interaction of electrons and ions, however, can never be neglected since ion charges, electron densities, charge imbalances, etc may change strongly during the FEL pulse. Besides that, the calculation of electron or ion spectra requires large propagation times because of the long range of the Coulomb interaction. Similar to methods applied for clusters in NIR pulses (Saalmann *et al* 2006), only *non-bound* electrons are propagated. These electrons are sometimes referred to as quasi-free or plasma electrons since, although released from the mother atom/ion ('inner ionization'), they may be bound to the cluster as a whole, cf section 2. Eventually, these electrons may be emitted from the cluster ('outer ionization'). Energy absorption, collision with other electrons and ions, and transient or permanent recombination of these electrons as well as ionic expansion are fully contained in the molecular dynamics calculation (Saalmann *et al* 2006, Jungreuthmayer *et al* 2005). The transition from bound to plasma electrons is treated by means of a Monte Carlo sampling (Georgescu *et al* 2007b) and requires rates to be discussed below.

In the second group of models, the various physical processes, such as photoionization (PI), inverse-bremsstrahlung (IBS) heating, collisional ionization and recombination, are treated independently using rates. These rates are adopted from known atomic cross sections, e.g. Lotz formulas for electron-impact ionization (Lotz 1968), or calculated in single-active-electron approaches, e.g. for IBS (Walters *et al* 2006). However, neighbouring ions may strongly perturb the nearby environment of the considered atom/ion, which is usually neglected for the rate calculation. Furthermore, photo-absorption and collision processes are considered as independent events in both time and space (Walters *et al* 2006). Plasma effects, however, are taken into account by artificially shifting ionization thresholds (Ziaja *et al* 2008), by considering Debye screening (Santra and Greene 2003) and as an input for electron-impact ionization. The density and temperature of the electron plasma are obtained by solving Boltzmann equations for electron and ion density distribution functions (Ziaja *et al* 2008) or by globally calculating them for the cluster (Walters *et al* 2006). The advantage of such approaches is their applicability to large cluster sizes, e.g. $N = 9 \times 10^4$ (Ziaja *et al* 2009b), which are inaccessible to molecular dynamics calculations.

There have been a number of implementations for both approaches. In particular, the calculations based on the rate approach differ in whether and how certain processes are taken into account. In order to validate theoretical approaches, often ion charge distributions are calculated and compared to measured data (Siedschlag and Rost 2004, Jungreuthmayer

et al 2005, Ziaja *et al* 2009b). Instead of presenting such comparisons, we concentrate in the following on the underlying physical mechanisms.

4. Clusters exposed to FLASH pulses

We discuss the nanoplasma dynamics in clusters related to experiments performed at FLASH which covered frequencies from $\hbar\omega \approx 12$ eV (early experiments) to $\hbar\omega \approx 90$ eV (recent experiments). A detailed description of these experiments is given in this issue (Bostedt and Möller 2010). These two frequencies induce very different processes and are characteristic of the VUV and XUV regimes, respectively.

4.1. Energy absorption

At the very first measurements at the Hamburg FEL (Wabnitz *et al* 2002), the laser frequency was $\hbar\omega = 12.7$ eV. This is slightly larger than the first ionization potential of xenon $E_{Xe} = 12.1$ eV, but smaller than the ionization potentials of higher charge states, e.g. $E_{Xe^+} = 21.0$ eV and $E_{Xe^{2+}} = 32.1$ eV (Lide 2010). Despite these large ionization potentials, time-of-flight spectra have clearly shown charge states as high as Xe^{8+} for the large clusters Xe_N with $\langle N \rangle \approx 3 \times 10^4$. Since a smaller cluster with $\langle N \rangle \approx 20, \ldots, 80$ did not produce such highly charged ions, it was clear that a 'cluster effect' has to be responsible for the particular efficient absorption of energy from the VUV laser pulse.

Highly charged ions (also with even higher charges) from laser-irradiated clusters have been observed before in experiments with intense NIR pulses (Ditmire *et al* 1997). There, resonant collective absorption of the nanoplasma dominates all other processes by far (Ditmire *et al* 1996, Saalmann 2006). The whole plasma is periodically driven in the background trapping potential and absorbs energy when the cluster eigenfrequency is resonant with the laser frequency. As individual collisions with ions are not relevant for the mechanism to work, it is sometimes referred to as collisionless absorption. At VUV or higher frequencies, however, the resonant collective absorption of the nanoplasma can be ruled out since the plasma eigenfrequencies are typically a few electron volts only and thus much smaller. Besides this, the quiver amplitude in the VUV field is much smaller than typical cluster radii, cf equation (2) and its discussion. Therefore, it was surprising that, despite the absence of the most important absorption mechanism of laser–cluster interaction, highly charged ions were detected. These surprising observations immediately sparked theoretical studies (Santra and Greene 2003, Siedschlag and Rost 2004, Rusek and Orłowski 2005, Jungreuthmayer *et al* 2005) aiming at understanding the underlying mechanism.

There are basically two processes by which clusters can *absorb* photons and thus energy: PI and IBS. In PI, a bound electron is promoted to a continuum state by the absorption of a photon. Correspondingly, IBS describes the photo-absorption of a free electron (Kroll and Watson 1973) which becomes possible only during collision with an ion. Cross sections for both processes can, in principle, be calculated in first order

with transition matrix elements between the initial (ψ_i) and final (ψ_f) states as

$$\sigma = 4\pi^2 \alpha / \omega^3 \, |\langle \psi_f | \partial V(r)/\partial z | \psi_i \rangle|^2, \qquad (5)$$

with $V(r)$ denoting the spherical atomic/ionic potential. The acceleration form used in equation (5) reveals that a steep slope of the potential V leads to large cross sections for PI and IBS. For first-order processes the energy of initial and final states differs by the energy of one photon: $E_f = E_i + \hbar\omega$. The cross sections (5) are determined, besides the shape of the potential, by initial and final states. For PI, the initial state ψ_i is a bound state; for IBS, both states are continuum states of free electrons and one has to sum over all possible states, i.e. with different angular momenta (Walters *et al* 2006). The challenge in calculating the cross sections and hence the corresponding rates consists in finding a reasonable approximation for the involved states. This is particularly difficult due to strongly perturbing neighbouring ions, which may considerably modify ionization potentials as well as orbitals.

At VUV frequencies, electrons are removed from the atoms/ions 'outside-in' like the shells of an anion because the ionization of inner-shell electrons would require multi-photon processes which are unlikely at the applied laser intensities. The fact that ionization can occur for charged ions, despite $\hbar\omega < E_{Xe^{q+}}$, is due to a modified 'continuum' in the cluster (Siedschlag and Rost 2004). The neighbouring ions lower the ionization potentials, whereby it turned out that in any charge step the resulting barriers are sufficiently low to allow for single-photon ionization into the quasi-continuum. In the original proposal (Siedschlag and Rost 2004), the influence of the electron plasma has been completely neglected. Its consideration, which has been achieved through coarse-graining the ultra-fast electron dynamics in time in order to calculate transient ion charge states (Georgescu *et al* 2007b), only slightly changes this picture. Since the typical temperatures of the electron plasma are about 10 eV or less (Ziaja *et al* 2009a), cf also figure 3(c), many electrons are (temporarily) localized at the ionic cores and screen them. A careful analysis of this electron localization, combined with the calculations of PI cross sections for equivalent electronic configurations, revealed that single-photon ionization is possible for the complete upper shell of the atoms (Georgescu *et al* 2007b). The resulting high electron density in the plasma (figure 3(b)) leads to an efficient heating by IBS, which explains the large amount of energy absorbed by the clusters. Figure 3(a) shows the IBS contribution as the difference between total absorbed energy and energy absorbed by PI. Note that, in the case of $\hbar\omega = 13$ eV (Siedschlag and Rost 2004), this contribution is much larger.

Alternatively, it has been proposed that the absorbed energy is not due to the high electron density but due to a particular efficient IBS (Santra and Greene 2003, Walters *et al* 2006). Instead of applying a simple Coulomb potential, as usually done in plasma physics (Shima and Yatom 1975), a modified potential $V(r)$ was used for the calculation of IBS according to equation (5). This potential accounts for the changes close to the nucleus, which are taken into account
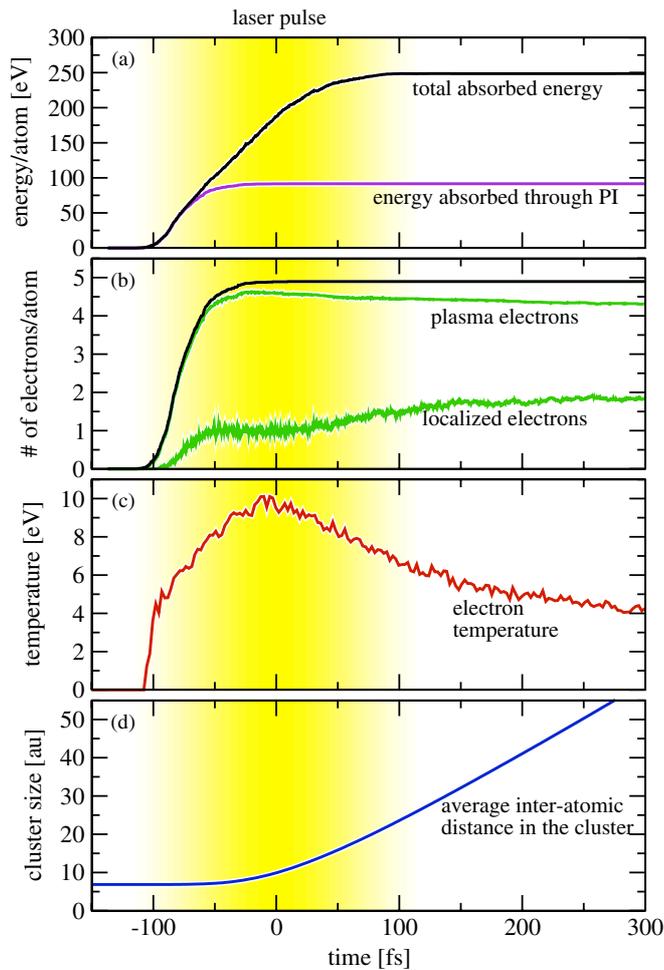
Figure 3. Typical scenario of VUV–cluster interaction. Dynamics of Ar_{147} exposed to a 20 eV FEL pulse with intensity $I = 7 \times 10^{13}$ W cm^{-2} and duration $T = 100$ fs, which is marked by the yellow/light-grey shaded area. From top to bottom: (a) total absorbed energy and energy absorbed through PI, (b) total electron number, number of plasma and transiently localized electrons, (c) electron temperature and (d) cluster size. Data from Georgescu *et al* (2007b).

with a parametrized (Santra and Greene 2003) or a modified Herrman–Skillman pseudo-potential (Walters *et al* 2006). These potentials coincide for large r with a Debye-screened Coulomb potential of a q-fold charged ion $V(r \to \infty) = -q \exp(-r/\lambda_D)/r$ with the Debye screening length λ_D. But they are much deeper at the nucleus $V(r \to 0) = -Z/r$ with the nuclear charge $Z \gg q$. Although the potentials are modified for small values $r \lesssim 1$ Å only, the IBS rates are sometimes increased by orders of magnitude (Santra and Greene 2003, Walters *et al* 2006). Calculations were done for free atoms without any (charged) environment. IBS heats the nanoplasma up to temperatures where, due to electron-impact ionization, high charge states are produced. Interestingly, the required temperatures are considerably higher than those measured by photo-electron spectroscopy (Laarmann *et al* 2005).

The calculated ion charge distributions of both approaches have shown good agreement with experimental data (Siedschlag and Rost 2004, Ziaja *et al* 2009b). Thus, more

refined experiments, e.g. the time-resolved measurement of transient ion charge states as discussed in the outlook, are necessary.

4.2. Relaxation and cluster explosion

Due to the multiple charging of the clusters, they undergo fragmentation. The expansion typically becomes relevant at a few tens of femtoseconds, cf figure 3(d), depending on the charge states and mass of the atomic species. Thus the heated plasma may cool down due to expansion during the laser pulses, as can be seen in figure 3(c). In contrast to NIR pulses, where the laser drives the plasma through the whole cluster and diminishes charge imbalances, here the electron plasma is 'confined' to the centre of the cluster. Thus the central part is screened and the charge accumulates at the surface (Siedschlag and Rost 2004, Ziaja *et al* 2008). Therefore, outer ionic shells are the first to expand, whereby the neutralized inner part survives much longer. During the expansion, electron–ion recombination lowers ionic charge states, which is relevant to quantitative comparisons with measured ion spectra.

Unfortunately, a theoretical description of this situation is difficult since very different time and length scales are involved, e.g. propagation methods are not able to track the dynamics on a picosecond or even a nanosecond time scale. Therefore, recombination during the cluster explosion is hardly investigated. An alternative to study the relaxation dynamics is pump–probe measurements (cf also section 5), which will become available in future beam times at FLASH.

4.3. Strong XUV laser pulses

The lasing mechanism of FEL machines allows us to change the frequency easily. Over recent years, the available frequency at FLASH has steadily increased (Ackermann *et al* 2007), starting from about $\hbar\omega = 12$ eV to about $\hbar\omega = 90$ eV. For experiments with clusters, this has dramatic consequences. First, new channels become accessible, e.g. when the photon frequency exceeds an ionization potential. Secondly, photo-absorption cross sections (for PI and IBS) depend critically on the wavelength, e.g. the PI cross section scales asymptotically with $\omega^{-7/2}$ (Bransden and Joachain 2003). Similarly, IBS cross sections decrease for larger frequencies and scales as $\omega^{-11/3}$ and ω^{-3} (Krainov 2000) for slow and fast electrons, respectively. Altogether, clusters become much less reactive for larger photon energies, i.e. nanoplasma formation is suppressed. Indeed, experiments measuring electron spectra from argon clusters at $\hbar\omega = 40$ eV (Bostedt *et al* 2008) have shown that a nanoplasma is formed only for the highest intensity. The fact that there is no nanoplasma for all other intensities was deduced from the fact that the electron spectra could be fully explained with an independent-electron model (Bostedt *et al* 2008). This model takes into account the gradual or multi-step charging of the cluster resulting in a flat electron spectrum.

Very recent FLASH experiments with xenon clusters at $\hbar\omega = 90$ eV (Bostedt *et al* 2010) have shown that this trend can be reversed. Due to the giant resonance of the 4d shell in xenon around 90 eV, which is connected with a large cross

section (Haensel *et al* 1969), PI becomes by far the dominating process of photon absorption. The formed dense nanoplasma becomes 'visible' through the emission of fast electrons in a process termed collisional auto-ionization (Bostedt *et al* 2010).

5. Outlook

The interest in experiments with clusters in short-wavelength intense FEL pulses will certainly continue. At the moment, several proposals for measurements at FLASH or LCLS are submitted or planned. On one hand, new and more detailed experimental data, e.g. by using so far inaccessible frequencies, performing pump–probe measurements or studying composite clusters, will be in need of theoretical support. On the other hand, more differential measurement will stimulate more refined theoretical descriptions.

We will conclude with mentioning the most interesting measurements to be performed in future FEL experiments. These are theoretical proposals for experiments as well as first experimental realizations to be continued in forthcoming beam times.

5.1. Clusters irradiated with x-ray pulses

As discussed above, IBS becomes inefficient at higher frequencies. However, new channels are opened for PI. Additionally, due to the fast charging of the cluster 'field ionization' from the cluster surface becomes important, cf section 2. Nanoplasma formation occurs by trapping, as shown in figure 2. It is therefore of particular interest to understand the time scale of this formation since efforts towards coherent diffractive single-molecule imaging (Gaffney and Chapman 2007) may be rendered impossible through an ultra-fast explosion of the sample, which could be slowed down by the formed plasma. Since the plasma 'settles' at the sample's centre, one could think of using a sacrificial layer which itself explodes but delivers electrons such that the sample of interest keeps its initial shape. Such a layer, also called tamper, was proposed recently for bio-molecules embedded in water (Hau-Riege *et al* 2007). Taking the 'field ionization' effect into account, the same result can be achieved also for clusters embedded in helium droplets despite the fact that helium is almost transparent for x-ray radiation and can only be ionized by the embedded core (Gnodtke *et al* 2009).

5.2. Pump–probe investigations

As discussed in section 4, the interpretation of the experimental results is still somewhat controversial. Pump–probe measurements are one way to discriminate between the different theoretical scenarios. Such experiments are already possible and are steadily improved at FLASH (Azima *et al* 2009). With respect to the nanoplasma dynamics, it would be interesting to trace the ionization stage of the cluster ions. This could be done through measuring kinetic energy spectra of the photo electrons from time-delayed pulses, either from an attosecond HHG or from a (shorter wavelength) FEL source. The technical realization of such a scheme is challenging.

However, it would provide time-resolved information of a multi-electron process which cannot be retrieved from energy-resolved observables. Calculations based on a molecular dynamics approach (Georgescu *et al* 2007a) have shown the feasibility of such an approach, provided the interaction of the probe pulse is weak and, therefore, acts as a small perturbation. Furthermore, the 'probe electron' should not undergo inelastic collisions and should be fast enough to be distinguished from the other emitted electrons. This requires higher photon frequencies for the probe pulses compared to the pump pulse and can only be applied to small clusters.

Another tool for probing the transient plasma state (Siedschlag and Rost 2005) is a short NIR pulse, which drives collective ionization (Saalmann and Rost 2003). Thereby the average ion charge in the cluster can be traced.

5.3. Composite clusters

Composite clusters, i.e. clusters formed by at least two types of atoms, introduce a new degree of freedom which on the one hand may enrich the dynamics, as for NIR frequencies (Mikaberidze *et al* 2009), but on the other hand allows for obtaining information which can be helpful in understanding the reaction of homo-nuclear clusters. First FEL experiments with core-shell systems made it possible to study the charge transfer dynamics inside clusters (Hoener *et al* 2008, Ueda 2010).

Acknowledgments

References

Ackermann W *et al* 2007 *Nature Photon.* **1** 336
Azima A *et al* 2009 *Appl. Phys. Lett.* **94** 144102
Barnes J E and Hut P 1986 *Nature* **324** 446
Bethe H A and Salpeter E 1957 *Quantum Mechanics of One- and Two-Electron Atoms* (Berlin: Springer)
Bostedt C *et al* 2010 *J. Phys. B: At. Mol. Opt. Phys.* **43** 194011 (this issue)
Bostedt C *et al* 2009 *Nucl. Instrum. Methods Phys. Res.* A **601** 108
Bostedt C *et al* 2008 *Phys. Rev. Lett.* **100** 133401
Bostedt C, Thomas H, Hoener M, Möller T, Saalmann U, Georgescu I, Gnodtke C and Rost J M 2010 to be published
Bransden B H and Joachain C J 2003 *Physics of Atoms and Molecules* (New York: Benjamin-Cummings)
Dachsel H 2010 *J. Chem. Phys.* **132** 119901
Ditmire T, Donnelly T, Rubenchik A M, Falcone R W and Perry M D 1996 *Phys. Rev.* A **53** 3379
Ditmire T, Tisch J W G, Springate E, Mason M B, Hay N, Smith R A, Marangos J and Hutchinson M H R 1997 *Nature* **386** 54
Faisal F H M 1987 *Theory of Multiphoton Processes* (New York: Plenum)
Fukuzawa H *et al* 2009 *Phys. Rev.* A **79** 031201
Gaffney K J and Chapman H N 2007 *Science* **316** 1444
Georgescu I, Saalmann U and Rost J M 2007a *Phys. Rev. Lett.* **99** 183002

Georgescu I, Saalmann U and Rost J M 2007b *Phys. Rev.* A **76** 043203

Gnodtke C, Saalmann U and Rost J M 2009 *Phys. Rev.* A **79** 041201

Greengard L and Rokhlin V 1987 *J. Comput. Phys.* **73** 325

Haberland H (ed) 1994 *Clusters of Atoms and Molecules Springer Series in Chem. Phys.* vols 52 and 56 (Berlin: Springer)

Haensel R, Keitel G, Schreiber P and Kunz C 1969 *Phys. Rev.* **188** 1375

Hau-Riege S P, London R A, Chapman H N, Szöke A and Tîmneanu N 2007 *Phys. Rev. Lett.* **98** 198302

Hoener M, Bostedt C, Thomas H, Landt L, Eremina E, Wabnitz H, Laarmann T, Treusch R, de Castro A R B and Möller T 2008 *J. Phys. B: At. Mol. Opt. Phys.* **41** 181001

Joachain C J, Dörr M and Kylstra N J 2000 *Adv. At. Mol. Opt. Phys.* **42** 226

Jungreuthmayer C, Ramunno L, Zanghellini J and Brabec T 2005 *J. Phys. B: At. Mol. Opt. Phys.* **38** 3029

Keldysh V 1965 *Sov. Phys.—JETP* **20** 307

Krainov V P 2000 *J. Phys. B: At. Mol. Opt. Phys.* **33** 1585

Krainov V P and Smirnov M B 2002 *Phys. Rep.* **370** 237

Kroll N M and Watson K M 1973 *Phys. Rev.* A **8** 804

Laarmann T, Rusek M, Wabnitz H, Schulz J, de Castro A R B, Gürtler P, Laasch W and Möller T 2005 *Phys. Rev. Lett.* **95** 063402

Last I and Jortner J 1999 *Phys. Rev.* A **60** 2215

Lide D R 2010 *CRC Handbook of Chemistry and Physics* (Boca Raton, FL: CRC Press/Taylor and Francis)

Lotz W 1968 *Z. Phys.* **216** 241

McPherson A, Thompson B D, Borisov A B, Boyer K and Rhodes C K 1994 *Nature* **370** 631

Mikaberidze A, Saalmann U and Rost J M 2009 *Phys. Rev. Lett.* **102** 128102

Rusek M and Orłowski A 2005 *Phys. Rev.* A **71** 043202

Saalmann U 2006 *J. Mod. Opt.* **53** 173

Saalmann U, Georgescu I and Rost J M 2008 *New J. Phys.* **10** 025014

Saalmann U and Rost J M 2002 *Phys. Rev. Lett.* **89** 143401

Saalmann U and Rost J M 2003 *Phys. Rev. Lett.* **91** 223401

Saalmann U, Siedschlag C and Rost J M 2006 *J. Phys. B: At. Mol. Opt. Phys.* **39** R39

Santra R and Greene C H 2003 *Phys. Rev. Lett.* **91** 233401

Shima Y and Yatom H 1975 *Phys. Rev.* A **12** 2106

Siedschlag C and Rost J M 2004 *Phys. Rev. Lett.* **93** 043402

Siedschlag C and Rost J M 2005 *Phys. Rev.* A **71** 031401

Springate E, Aseyev S A, Zamith S and Vrakking M J J 2003 *Phys. Rev.* A **68** 053201

Ueda K 2010 private communication

Wabnitz H *et al* 2002 *Nature* **420** 482

Walters Z B, Santra R and Greene C H 2006 *Phys. Rev.* A **74** 043204

Ziaja B, Laarmann T, Wabnitz H, Wang F, Weckert E, Bostedt C and Möller T 2009a *New J. Phys.* **11** 103012

Ziaja B, Wabnitz H, Wang F, Weckert E and Möller T 2009b *Phys. Rev. Lett.* **102** 205002

Ziaja B, Wabnitz H, Weckert E and Möller T 2008 *New J. Phys.* **10** 043003

Zweiback J, Ditmire T and Perry M D 1999 *Phys. Rev.* A **59** R3166